Journal of Inorganic Biochemistry 191 (2019) 112–118

Contents lists available at ScienceDirect

Journal of Inorganic Biochemistry

journal homepage: www.elsevier.com/locate/jinorgbio

Novel structures of platinum complexes bearing *N*-bisphosphonates and study of their biological properties

Amparo Alvarez-Valdes[a], Ana I. Matesanz[a], Josefina Perles[b], Célia Fernandes[c], João D.G. Correia[c], Filipa Mendes[c,*], Adoracion G. Quiroga[a,*]

[a] Inorganic Chemistry Department, Universidad Autónoma de Madrid, 28049, Spain
[b] SIdI (Servicio Interdepartamental de Investigación), Universidad Autónoma de Madrid, 28049, Spain
[c] Centro de Ciências e Tecnologias Nucleares, Instituto Superior técnico, Universidade de Lisboa, CTN, Estrada Nacional 10 (km 139,7), 2695-066 Bobadela LRS, Portugal

ARTICLE INFO

Keywords:
Platinum complexes
Bisphosphonates
DNA
Hydroxyapatite

ABSTRACT

Novel bisphosphonate platinum complexes: $[Pt(isopropylamine)_2(BP)]NO_3$ (BP = pamidronate and alendronate) have been synthesized and characterized. Their monomeric structure contains a bisphosphonate acting as chelate ligand through its oxygen atom donors, conferring the compound's cationic structure with a good solubility in water. The study of the compounds in solution showed high stability up to 24 h. The cytotoxicity in cancer cell lines has been assessed. We also present preliminary studies on the evaluation of the affinity towards biological targets such as DNA (both calf thymus DNA and supercoiled plasmid DNA) and hydroxyapatite where the complexes showed a low DNA interaction, but a clear affinity for hydroxyapatite comparing to their precursors.

1. Introduction

Bisphosphonates (BPs) belong to a family of drugs indicated for the treatment of pathologic conditions characterized by increased osteoclast-mediated bone resorption, namely Paget's disease, osteoporosis and tumor bone disease [1–3]. BP's bind strongly to hydroxyapatite (HAP), the main component of the inorganic matrix of bone, and such affinity is due to the chelation to Ca^{2+} ions. The biological properties of BPs are assigned to the cellular effects caused on osteoclasts, and it has been shown that the nature of the substituents on the basic structure of the BP is determinant for their potency in terms of inhibition of bone resorption [4].

Studies suggest that BPs may also present antitumoral activity, however, such finding must still be fully confirmed in the clinical setting [5,6]. More importantly, BP's are also being evaluated for their ability to selectively deliver anticancer drugs to bone metastases [7], with the aim of achieving a reduction of the severe side effects associated to most systemic chemotherapeutic agents used in the clinical setting.

Cisplatin is still one of the most potent agents currently used in cancer chemotherapy. However, patients experience severe side effects, which have guided the investigations towards non-conventional platinum complexes [8]. Within the several distinct strategies described in the literature for the development of improved platinum-based cytotoxic drugs, there are a few examples of “targeting” the drug specifically to the bone using a BP. Studies on this topic have shown that the antiproliferative effect of phosphonate-containing platinum(II) complexes [9] was not improved over cisplatin's, but the complexes were more active than their BP ligand precursors. Subsequent studies with these complexes confirmed a superior therapeutic activity in transplanted rat osteosarcoma models [10–12].

The third generation of platinum drugs (oxaliplatin, and carboplatin) induces DNA adducts [13] which are, in average, more cytotoxic than those induced by cisplatin. Therefore, oxaliplatin analogues with phosphonates [12] were investigated expecting that the structural modification would translate into even more favorable pharmacological properties than those described for oxaliplatin. The values of cytotoxicity found in this novel series of complexes were higher than cisplatin and oxaliplatin (and consequently less cytotoxic) but the compounds showed an improved cytotoxicity compared to the phosphonate itself, proving that the proposed approach is valid. All these examples are monomeric structures, where the BPs coordinate via nitrogen and oxygen, and the highly charged oxygen of the BPs are free to interact with their potential targets.

The interest in platinum BP derivatives has also motivated the development of biomimetic apatite nanocrystals for potential use in bone

* Corresponding authors.
E-mail addresses: fmendes@ctn.tecnico.ulisboa (F. Mendes), adoracion.gomez@uam.es (A.G. Quiroga).

https://doi.org/10.1016/j.jinorgbio.2018.11.010
Received 31 July 2018; Received in revised form 22 October 2018; Accepted 16 November 2018
Available online 18 November 2018
0162-0134/

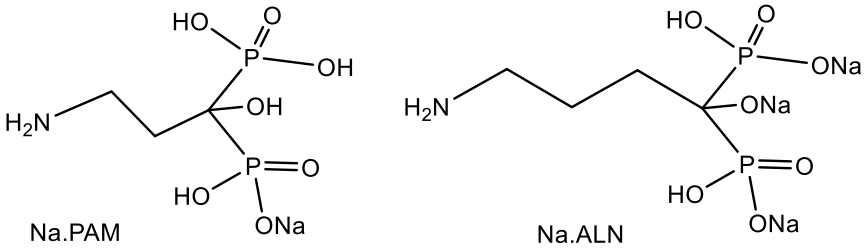

Fig. 1. Chemical structure of the BPs used for this work.

implantation, which can act as a local targeted delivery system for anticancer and anti-metastatic drugs [14], without however surpassing the cytotoxicity of cisplatin [15].

With the aim of developing novel osteotropic platinum(II) complexes potentially useful for treating bone metastatic disease and/or to avoid the severe side effects linked to systemic treatments, we have synthesized and fully characterized two novel platinum(II) complexes of *cis* configuration, bearing an isopropylamine (ipa) and the nitrogen-containing BPs pamidronate(PAM) and alendronate(ALN) as chelating ligands (Fig. 1). Their antiproliferative properties in different cancer cell lines and their reactivity versus biological targets such as models of DNA were also studied.

2. Materials and methods

2.1. General procedures

Mono-dimensional ^{195}Pt NMR, ^{13}C NMR and ^{1}H NMR and ^{31}P NMR experiments were performed in DMSO-d_6 and D_2O using a Bruker AMX-300 (300 MHz) and DXR-500 spectrometer at room temperature (25 °C). Elemental analyses were performed on a Perkin Elmer 2400 Series II microanalyzer. Mass spectrometry assays were performed with a Hybrid Quad-Tof (QTOF) mass spectrometer: QSTAR (ABSciex) using fresh samples.

2.2. Synthesis and characterization of complexes

Cis-$PtI_2(ipa)_2$ was prepared following a procedure previously described [16]. A water solution (0.5 mL) of $AgNO_3$ (30 mg, 0.176 mmol) was added to an acetone solution (1.5 mL) of *cis*-$PtI_2(ipa)_2$ (50 mg, 0.088 mmol). The resulting mixture was stirred at room temperature in darkness. After 24 h, a pale yellow solid (AgI) was separated. The resulting solution was added to a water solution of either pamidronate (NaPAM) (24.2 mg, 0.088 mmol in 4 mL) or alendronate (NaALN) (34.1 mg, 0.088 mmol in 2 mL). The mixture was stirred at room temperature for 3 days. The final solution was concentrated, and the addition of acetone afforded a white solid, which was isolated by filtration, washed with acetone and dried under vacuum.

Complex 1, *cis*-$[Pt(ipa)_2(PAM)][Pt(ipa)_2(PAMH)]NO_3$. White solid. Yield 45%. Mass $[C_9H_{28}N_3O_7P_2Pt]^+$: 547.09 (calculated: 547.10) Elemental analysis $C_9H_{28}N_4O_{10}P_2Pt$: Calculated: C 17.74, H 4.63, N 9.19. Found: C 17.38, H 4.95, N 8.98%. ^{1}H NMR (D_2O) ppm: 1.3 d (12H); 2.2 m(2H); 2.9 sep(2H); 3.35 m(2H). ^{13}C NMR (D_2O) ppm: 22.3; 30.2; 36.0; 48.8; 75.4. ^{31}P NMR (D_2O) ppm: 26.8. ^{195}Pt NMR (D_2O) ppm: −1622. Single crystal suitable for X-ray diffraction was grown from a water/acetone solution.

Complex 2 *cis*-$[Pt(ipa)_2(ALN)][Pt(ipa)_2(ALNH)]NO_3$. White solid. Yield 40%. Mass $[C_{10}H_{30}N_3O_7P_2Pt]^+$: 561.1 (calculated: 561.1) Elemental analysis $[C_{10}H_{30}N_4O_{10}P_2Pt]$ Calculated: C 19.27, H 4.85, N 8.99. Found: C 19.61, H 4.72, N 8.65%. ^{1}H NMR (D_2O) ppm: 1.4 d (12H); 2.1 m(4H); 3.0 sep(2H); 3.1 m(2H). ^{13}C NMR (D_2O) ppm: 22.4; 30.0; 39.8; 48.6; 75.4; 82.2. ^{31}P NMR (D_2O) ppm: 27.3. ^{195}Pt NMR (D_2O) ppm: −1613.

2.3. Single crystal X-ray diffraction

A suitable colourless crystal of **1** was coated with mineral oil and mounted on a Mitegen MicroMount. The sample was transferred to a Bruker Kappa Apex II diffractometer equipped with graphite monochromated Mo Kα radiation (λ = 0.71073 Å). Full details of the data collection and refinement can be found in the Supplementary material. Raw intensity data frames were integrated with the SAINT program [17], which also applied corrections for Lorentz and polarization effects. Empirical absorption corrections were subsequently applied (SADABS) [18]. The Bruker SHELXTL Software Package was used for space group determination, structure solution, and refinement [19]. The space group determination was based on a check of the Laue symmetry, and systematic absences were confirmed using the structure solution. The structures were solved by direct methods (SHELXS-97), completed with different Fourier syntheses, and refined with full-matrix least-squares using SHELXS-97 minimizing $\omega(F_o^2 - F_c^2)^2$. Weighted R factors (R_w) and goodness of fit are based on F^2 while conventional R factors (R) are based on F. All non-hydrogen atoms were refined with anisotropic displacement parameters. Hydrogen atoms were calculated geometrically and allowed to ride on their parent carbon atoms with fixed isotropic U. All scattering factors and anomalous dispersion factors are contained in the SHELXTL 6.10 program library. The crystal structure of compound **1** has been deposited at the Cambridge Crystallographic Data Centre with code CCDC 997272.

2.4. Stability assays

The stability of complexes **1** and **2** was evaluated by UV/Vis spectrophotometry at 37 °C and NMR spectroscopy. For the UV/Vis studies, complexes **1** and **2** were dissolved in water or Tris buffer (NaCl 50 mM, Tris-HCl 5 mM, pH was adjusted to 7.1 with NaOH 0.5 M) to obtain 1 mM concentration and the absorbance, at the corresponding λ max established for each compound, was measured over 24 h. For the NMR spectroscopy assay, about 1,5 mg of each complex was dissolved in 0.7 mL D_2O and the ^{1}H NMR was measured versus time.

2.5. Cytotoxicity assays

2.5.1. Cell culture

The human ovarian cancer cell lines A2780 and A2780cisR (resistant to cisplatin) and the human prostate cancer cell line PC3 were grown in RPMI 1640 culture medium (Invitrogen) supplemented with 10% fetal bovine serum (FBS) and 1% penicillin/streptomycin at 37 °C in a humidified atmosphere of 95% of air and 5% CO_2 (Heraeus, Germany). The human breast cancer cell line MDAMB231 was grown in Dubelcco's modification of Eagle medium (DMEM) culture medium (Invitrogen) supplemented with 10% FBS and 1% penicillin/streptomycin, in similar conditions as above.

2.5.2. Cytotoxicity assay

The cytotoxicity of the complexes was assessed in the A2780, its cisplatin-resistant variant (A2780cisR), PC3 MDAMB231 cell lines, using a colorimetric method based on the tetrazolium salt MTT

([3-(4,5-dimethylthiazol-2-yl)-2,5-diphenyltetrazolium bromide), which is reduced by viable cells to yield purple formazan crystals. Cells were seeded in 96-well plates at a density of 1×10^4 to 1.5×10^4 cells per well in 200 µL of culture medium and left to incubate overnight for optimal adherence. After careful removal of the medium, 200 µL of a dilution series of the compounds (stock solutions prepared fresh in water) in medium were added and incubation was performed at 37 °C/ 5% CO_2 for 72 h. At the end of the incubation period, the compounds were removed and the cells were incubated with 200 µL of MTT solution (500 µg/mL). After 3–4 h at 37 °C/5% CO_2, the medium was removed and the purple formazan crystals were dissolved in 200 µL of DMSO by shaking. The cell viability was evaluated by measurement of the absorbance at 570 nm using a plate spectrophotometer (Power Wave Xs, Bio-Tek). The cell viability was calculated dividing the absorbance of each well by that of the control wells. Each point was determined in at least 4 replicates in 3 independent assays.

2.6. DNA interaction experiments

2.6.1. UV/ Vis spectroscopy with CT-DNA

A calf thymus (CT)-DNA (supplied by Aldrich-Sigma) stock solution was prepared by dissolving the lyophilized sodium salt in Tris buffer by stirring for 5 h. The CT-DNA solution was determined spectrophotometrically by using its known molar absorbance coefficient at 260 nm (6600 $M^{-1} \cdot cm^{-1}$). The ratio of UV absorbance at 260 and 280 nm, A260/A280, was ca. 1.9, indicating that the DNA was sufficiently free of protein. The stock solution was kept frozen until the day of the experiment. Spectrophotometric titrations were performed at a fixed DNA concentration ($5 \cdot 10^{-5}$ M) and increasing concentrations of the compounds (r_c = [CT-DNA] / [compound]) and monitored by absorbance at 260 nm.

2.6.2. Plasmid DNA interaction

DNA aliquots containing 8 µL of the model plasmid DNA-pBR322 (10 ng/mL stock) in 10 mM Tris-HCl (pH 7.6) and 1 mM EDTA were incubated with the platinum compounds at several r_i (r_i = [complex] / [nucleotide]) values (0.001 to 0.5). The stock solutions of the platinum complexes (5 µM or 50 µM) were prepared in water and used fresh.

The samples were incubated at 37 °C for 24 h, after which time 2 µL of a loading dye containing 50% glycerol, 0.25% bromophenol blue and 0.25% xylene cyanol was added. The total of the sample (20 µL) was loaded in the wells of a 0.8% agarose gel. Electrophoresis was carried out for a period of 2.5 h at approximately 50 V. After electrophoresis the gel was immersed in 800 mL of Millipore water containing 64 µL of a 10 mg/mL stock solution of ethidium bromide for 30 min to stain the DNA. Finally, the stained gel was analyzed with a UVITEC Cambridge with a UVIDOC HD2.

2.7. HPA interaction experiments

Hydroxyapatite (nanopowder < 200 nm particle size BET > 97% synthetic) was purchased from Aldrich (677418). One set of samples for the binding experiments were prepared by dissolving 1,3 mg of the ligand PAM in a 0.5 mL of Tris-HCl (pH 7.5) and 10% D_2O (150 mM). Another set of samples were prepared by dissolving 1,3 mg of the ligand PAM in 0.5 mL of D_2O and 1.4 mg of complex **1** in 0.5 mL of D_2O. The samples were incubated with HAP (0.2–0.6 mg) for 5 min. and centrifuged. No differences were detected in the PAM analysis compared to the reported spectra (Fig. SI1). The samples were analyzed by one dimensional ^1H NMR with a Bruker DRX500 instrument with water suppression and following the procedure published before [20]. The total measuring time for each sample was around 25 min and trimethylsilylpropanoic acid (TSP) was used into the sample as a 0 ppm reference.

3. Results

3.1. Synthesis and characterization of platinum complexes with phosphonate and isopropylamine

The structural design of the complexes presented here was envisaged towards the possible application bisphosphonate-containing complexes of active platinum complexes bearing isopropylamine (such as iproplatin [8] and/or *trans* complexes with isopropylamine) as osteotropic platinum(II) complexes potentially useful for treating bone metastatic disease.

The parent platinum complex, *cis*-$PtI_2(ipa)_2$ was selected because of its interesting and unconventional biological properties [16,21]. BPs were chosen for the specific interaction in bone metastasis and for the nitrogen-containing structures; pamidronate (NaPAM) and alendronate (NaALN) [22]. The complexes were prepared using a metathesis reaction of *cis*-Pt(isopropylamine)$_2X_2$ ($X = I^-$) with $AgNO_3$, allowing the reaction with PAM and ALN to afford the monomeric complexes, **1** and **2**, respectively. The reaction was performed at different conditions, such as varying the stoichiometric ratio Pt:BP and temperature. However, in all cases, the same monomeric compound was obtained as the major product.

The characterization of both complexes was performed by the usual analytical techniques, indicating the presence of one bisphosphonate molecule and two isopropylamine residues. All the data are compiled in the Supplementary information (SI). Brought together, the results obtained were in accordance with either general formulae: $[Pt(ipa)_2(BP-H)]$ and/or $[Pt(ipa)_2(BPH)]NO_3$. The core of the platinum cation is clearly observed in mass spectra, which in both cases (complex **1** and **2**) showed the molecular formula of B in solution (see Scheme 1) where the bisphosphonate might act as a chelating ligand through two oxygen atoms in a bidentate coordination mode.

The single crystal X-ray structure of compound **1** (Fig. 2) was in agreement with the formula $[Pt(ipa)_2(PAM)] / [Pt(ipa)_2(PAMH)]NO_3$. The asymmetric unit $[Pt(ipa)_2(BPH_{0.5})](NO_3)_{0.5}$ contains only one platinum complex (with 50% occupation for the hydroxylic hydrogen atom H7) and half of a nitrate anion, displaying interesting supramolecular interactions between them (see Table S3 for hydrogen bond interactions). An alternative model with a double asymmetric unit was tried, but it did not refine well against the experimental data, meaning that the two species $[Pt(ipa)_2(PAM)]$ and $[Pt(ipa)_2(PAMH)]^+$ are randomly distributed in the crystal. In the metal complex, there are also two alternative positions for oxygen atoms O1 to O6 in the phosphonate groups with 75%–25% occupation. Complex **2** was assigned as $[Pt(ipa)_2(ALN)] / [Pt(ipa)_2(ALNH)]NO_3$ based in the high similarities in the spectroscopic characterization.

The monomeric structures of complexes **1** and **2** are unique in the literature, as the published examples are in most of the cases dinuclear and polynuclear compounds [15,23]. The few monomeric examples described contain nitrogen-containing bisphosphonates (N-BP) coordinated to the Pt atom, as the one described by Guo and coworkers [24]. In this last example, the cleavage of the pendant bisphosphonate ester moiety of the N-coordinated ligand results in a non-stable platinum complex with a free bisphosphonic acid unit.

The stability of complexes **1** and **2** in water and Tris buffer was assessed by UV/Vis spectrophotometry at 37 °C and NMR spectroscopy (Figs. 3 and 4 respectively). The results obtained demonstrated that both compounds were unusually stable in aqueous solutions.

No hydrolysis of the bisphosphonate was detected when monitoring the solution by ^1H and ^{31}P NMR spectroscopy in D_2O for both complexes (Fig. 4) in the first 24 h. The behaviour of complexes **1** and **2** in water was monitored by ^{31}P NMR spectroscopy up to one week. Remarkably, only after long periods, some speciation could be detected. As an example, the ^{31}P NMR spectrum of complex **1** is shown in Fig. 4c, where two new species could be observed only after 7 days, which asserts the high stability of the complexes in aqueous solution.

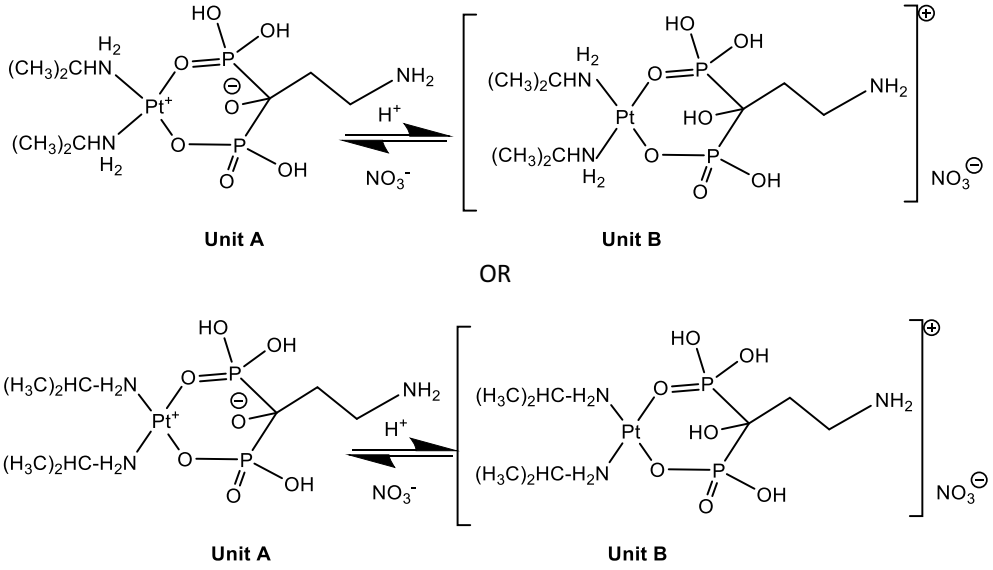

Scheme 1. Forms detected for complex **1** by ESI-mass and by NMR.

Interestingly these data show that herein we report the first crystal structure of a platinum complex where the bisphosphonate ligand is bound through most of the oxygen atoms, and that this unique example is both very soluble and remarkably stable in aqueous solutions.

3.2. Cytotoxicity evaluation

The antiproliferative properties of complexes **1** and **2** were assayed by monitoring their ability to inhibit cell growth. Cytotoxic activity was determined on the human ovarian cancer (A2780) cell line, its cisplatin-resistant variant (A2780cisR) and on the human prostate cancer (PC3) and breast cancer cell lines (MDAMB231), by a colorimetric method (MTT assay). A comparison between the activity of reference drug cisplatin, the precursor Pt(II) complex and the free BPs and the activity of these new metal compounds was performed in our cell models. Using an appropriate range of concentrations (200–0,1 μM), dose-response curves after long-term (72 h) exposure were obtained. From the experimental values, we have calculated the IC_{50} for the 4 compounds, presented in Table 1.

The free bisphosphonates NaPAM and NaALN showed moderate to low cytotoxicity. Complexes **1** and **2** presented even lower cytotoxicity, with complex **2** being more cytotoxic than complex **1**. Both, complex **2** and its free BP are more potent in the A2780cisR and MDA MB231 cells lines. We also tested cisplatin in the presence of complex **2** in A2780cisR in order to check for a synergistic effect in cell death (not shown). However, no increase in cell death was observed versus cisplatin alone.

3.3. Reactivity towards biological targets: study of interaction with DNA and HPA

Following the verification of the high stability of the complexes in aqueous solutions, the complexes were further evaluated in terms of their reactivity towards biological targets such as DNA and HPA.

We first studied the reaction of complex **1** with CT-DNA by UV/Vis spectrophotometry, as a simple assay to assess DNA binding. A titration of complex **1** with CT-DNA was followed by monitoring the characteristic $\pi \rightarrow \pi^*$ band at 260 nm (Fig. 5), typical of the B-form of DNA. In these studies, the addition of increasing amounts of **1** to a known concentration of CT-DNA (50 μM) produced no appreciable changes in the intensity of the DNA absorption, which suggests poor CT-DNA affinity.

In the literature, cisplatin and other Pt(II) complexes have been widely reported to produce changes in the mobility of the different isoforms of plasmid DNA in gel electrophoresis [8,9,25]. Therefore, the interaction of complex **1** with a model plasmid DNA, pBR322, was evaluated by monitoring the mobility in gel electrophoresis (Fig. 6). The plasmid DNA was incubated with different concentrations of

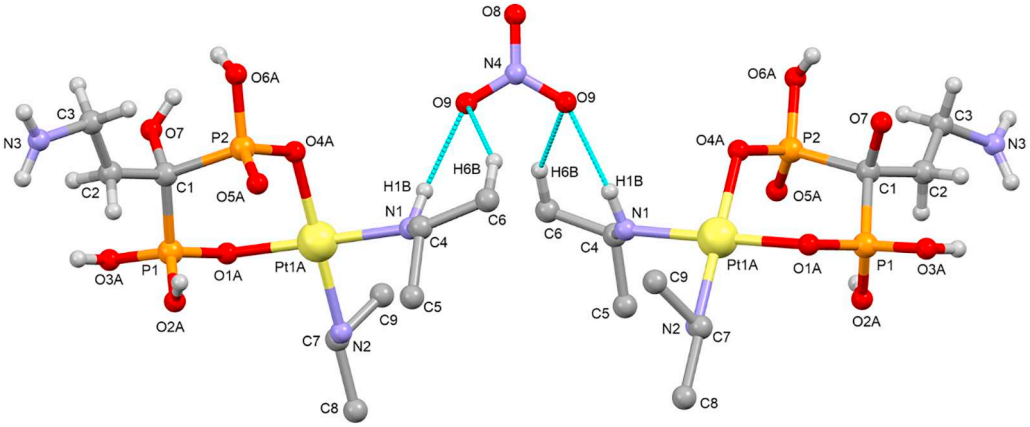

Fig. 2. Molecular plot obtained from SCXRD data of $[Pt(ipa)_2(BPs)][Pt(ipa)_2(BPsH)]NO_3$ (**1**), where interactions between two units and a nitrate anion are depicted in cyan. Hydrogen atoms in the ipa ligands not participating in hydrogen bonds have been removed for clarity.

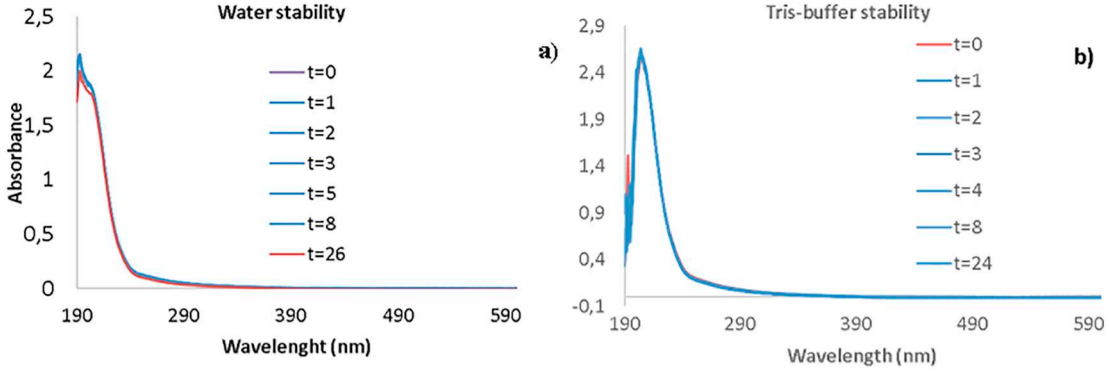

Fig. 3. UV absorption spectra of **1** from fresh to 24 h dissolved in a) water and b) Tris buffer.

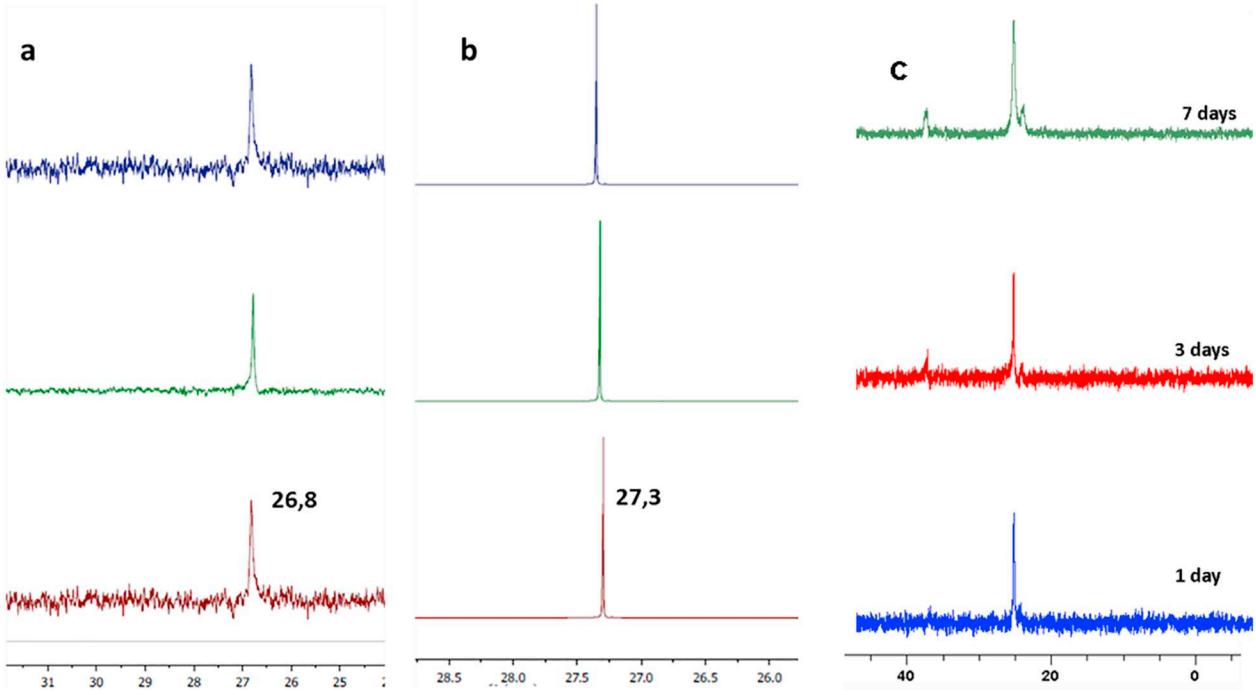

Fig. 4. ^{31}P NMR spectra of Pt-BP complexes. a) Stability of complex 1 in D_2O monitored at 1 h, 6 h and 24 h; b) stability of complex 2 in D_2O monitored at 1 h, 6 h and 24 h; c) stability of complex 1 in D_2O at longer time periods (1, 3 and 7 days).

Table 1
IC_{50} values in four different human cell lines (72 h incubation).

Compound	IC_{50} (μM)			
	A2780	A2780cisR	MDA MB231	PC3
NaPAM	59 ± 1.3	60.8 ± 1.1	134.9 ± 2.0	100 ± 2.0
1	> 200	> 200	> 200	> 200
NaALN	184.4 ± 2.2	74.4 ± 1.0	69.5 ± 2.3	107.6 ± 1.5
2	> 200	103 ± 1.2	100.2 ± 3.0	> 200
$Pt(ipa)_2I_2$	3.1 ± 1.5	5.9 ± 1.4	0.4 ± 0.2	1.8 ± 1.0
Cisplatin	2.3 ± 1.1	16.09 ± 1.5	3–10[a]	51 ± 2.5
Carboplatin	5–11[a]	4–40[a]	–	–

[a] Data from literature.

complex **1** expressed as r_i (complex **1**: DNA base pairs). The results obtained show that there is no alteration in the electrophoretic mobility of the isoforms of pBR322 when incubated with increasing amounts of complex **1**.

From both DNA interaction experiments, we can conclude that the DNA is not a target for this complex, and this might be related to the reduced cytotoxicity presented.

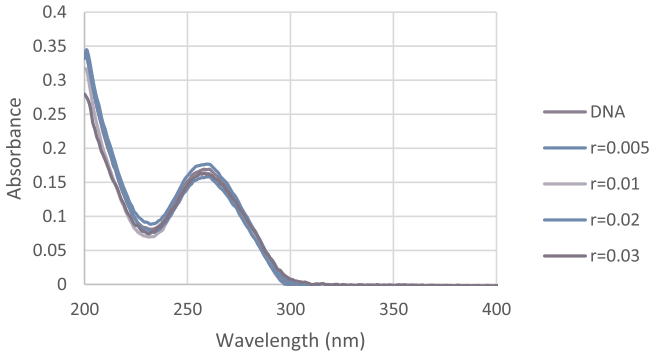

Fig. 5. UV absorption spectra of CT-DNA in the presence of increasing amounts of the complex **1** at diverse r_c (r_c = [CT-DNA] / [complex]).

The studies presented thus far show that complex **1** presents high stability in aqueous solution and poor interaction with DNA. Next, the potential binding affinity for bone was assessed.

There are three methods generally used to determine the bisphosphonate binding affinity for bone powder or HAP [26–28] but none of

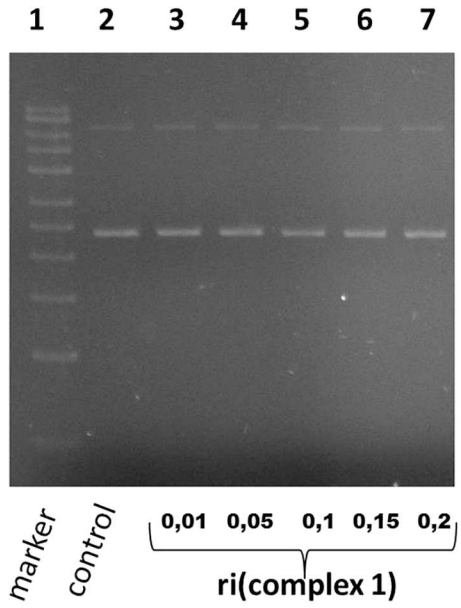

Fig. 6. Electrophoresis of plasmid DNA pBR322 after incubation with complex **1** at 37 °C for 24 h. Lane 1 – molecular weight marker, lane 2 – pBR322 Control (no complex), lanes 3–7 pBR322 incubated with increasing concentrations of complex **1**, ri = Complex:DNA (base pair) ratio.

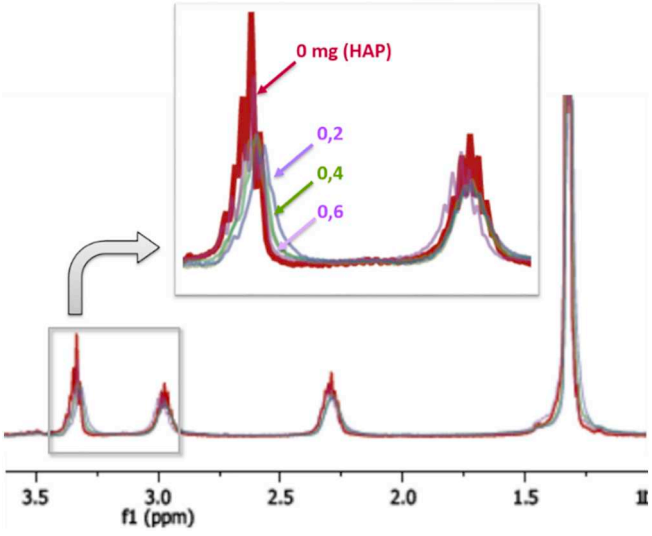

Fig. 7. HAP binding assay monitored by ^{1}H NMR spectroscopy.in the direct binding format to Complex **1** was incubated with increasing amounts of HAP (0, 0.2, 0.4, or 0.6 mg).

them is applicable to a wide range of binding affinities. Recently Jahnke et al. presented a NMR-based method that gives a solid evaluation for both binding to HAP and bone powder [20]. The assay allows the evaluation of strategies of targeting active substances selectively to the bone by tethering them a bone-affinity tag, and facilitates identification of suitable attachment points. In this investigation, we were especially interested in comparing the bone/HAP affinity of the BP NaPAM ligand (reported previously in the literature [20]) with the one of complex **1**. A binding assay to HAP was performed with NaPAM and complex **1** and NMR spectroscopy used to detect the possible interactions. Briefly, after incubation of the compounds with increasing concentrations of HAP, the samples were centrifuged, the supernatant collected and the intensity of the signals detected for NaPAM and complex **1** monitored by ^{1}H NMR spectroscopy. The experiment was performed using a 500 MHz NMR spectrometer, and in order to maximize the signal resolution a compound concentration higher than the published results (150 mM) was used. At first we performed the experiments using Tris solutions and water, with no differences, so water solutions were finally used in our methodology (see experimental part).

Although we could not quantify the binding affinity of the ligand or complex, we could confirm and detect that complex **1** maintains the BP affinity for HAP (Fig. 7) as the ^{1}H NMR signals decreased in the spectra, with the increasing of HAP concentration. This effect is also observed in the ligand NaPAM, which was quantified in a previous work [20] (Fig. SI1).

Taken together, all these experiments show that although these complexes do not show relevant cytotoxic activity or DNA affinity, their structure assures a remarkable solubility and stability in solution. This indicates that the new bisphosphonate complexes could be used in biological systems as a robust element without toxic effect. Moreover, our preliminary data shows that complex **1** presents affinity for HAP, a characteristic endowed by the BP moiety.

Abbreviations

BP	bisphosphonate
HPA	hydroxyapatite
ipa	isopropylamine
PAM	pamidronate
ALN	alendronate

Declaration of interest

None.

Funding

This work was supported by the Spanish MINECO grant CTQ2015-68779R. MetDrugs network is also acknowledged (A.A; A.I.M. and A.G.Q.). This work has been partially supported by the Fundação para a Ciência e a Tecnologia (FCT), Portugal, through the UID/Multi/04349/2013 project.

Appendix A. Supplementary data

Supplementary data to this article can be found online at https://doi.org/10.1016/j.jinorgbio.2018.11.010.

References

[1] E.F. Eriksen, A. Diez-Perez, S. Boonen, Bone 58 (2014) 126–135.
[2] L. Costa, Curr. Opin. Support. Palliat. Care 8 (2014) 414–419.
[3] L. Costa, Lancet Oncol. 15 (2013) 15–16.
[4] K.L. Kavanagh, K. Guo, J.E. Dunford, X. Wu, S. Knapp, F.H. Ebetino, M.J. Rogers, R.G.G. Russell, U. Oppermann, Proc. Natl. Acad. Sci. 103 (2006) 7829–7834.
[5] M.C. Winter, I. Holen, R.E. Coleman, Cancer Treat. Rev. 34 (2008) 453–475.
[6] M. Gnant, P. Clezardin, Cancer Treat. Rev. 38 (2012) 407–415.
[7] E. Palma, J.D.G. Correia, M.P.C. Campello, I. Santos, Mol. BioSyst. 7 (2011) 2950–2966.
[8] T.C. Johnstone, K. Suntharalingam, S.J. Lippard, Chem. Rev. 116 (2016) 3436–3486.
[9] M.J. Bloemink, B.K. Keppler, H. Zahn, J.P. Dorenbos, R.J. Heetebrij, J. Reedijk, Inorg. Chem. 33 (1994) 1127–1132.
[10] T. Klenner, F. Wingen, B. Keppler, P. Valenzuela-Paz, F. Amelung, D. Schmehl, Clin. Exp. Metastasis 8 (1990) 345–359.
[11] T. Klenner, F. Wingen, B.K. Keppler, B. Krempien, D. Schmehl, J. Cancer Res. Clin. Oncol. 116 (1990) 341–350.
[12] M. Galanski, S. Slaby, M.A. Jakupec, B.K. Keppler, J. Med. Chem. 46 (2003) 4946–4951.
[13] J.M. Woynarowski, S. Faivre, M.C.S. Herzig, B. Arnett, W.G. Chapman, A.V. Trevino, E. Raymond, S.G. Chaney, A. Vaisman, M. Varchenko, P.E. Juniewicz, Mol. Pharm. 58 (2000) 920–927.
[14] B. Palazzo, M. Iafisco, M. Laforgia, N. Margiotta, G. Natile, C.L. Bianchi, D. Walsh, S. Mann, N. Roveri, Adv. Funct. Mater. 17 (2007) 2180–2188.
[15] N. Margiotta, R. Ostuni, V. Gandin, C. Marzano, S. Piccinonna, G. Natile, Dalton Trans. (2009) 10904–10913.
[16] L. Messori, A. Casini, C. Gabbiani, E. Michelucci, L. Cubo, C. Ríos-Luci, J.M. Padrón,

C. Navarro-Ranninger, A.G. Quiroga, ACS Med. Chem. Lett. 1 (2010) 381–385.
[17] Bruker, SAINT, Bruker AXS Inc., Madison, Wisconsin, USA, 2012.
[18] Bruker, SADABS, Bruker AXS Inc., Madison, Wisconsin, USA, 2001.
[19] G.M. Sheldrick, Bruker AXS SHELXTL version 6.10, structure determination package, Bruker Analytical X-ray Instruments, 2000 (Madison, WI), Acta Cryst C71 (2015) 3–8.
[20] W. Jahnke, C.l. Henry, ChemMedChem 5 (2010) 770–776.
[21] L. Messori, T. Marzo, C. Gabbiani, A.A. Valdes, A.G. Quiroga, A. Merlino, Inorg. Chem. 52 (2013) 13827–13829.
[22] E. Palma, J.o.D.G. Correia, B.L. Oliveira, L. Gano, I.C. Santos, I. Santos, Dalton Trans. 40 (2010) 2787–2796.
[23] N. Margiotta, F. Capitelli, R. Ostuni, G. Natile, J. Inorg. Biochem. 102 (2008) 2078–2086.
[24] Z. Xue, M. Lin, J. Zhu, J. Zhang, Y. Li, Z. Guo, Chem. Commun. 46 (2010) 1212–1214.
[25] A.G. Quiroga, J.M. Perez, E.I. Montero, J.R. Masaguer, C. Alonso, C. Navarro-Ranninger, J. Inorg. Biochem. 70 (1998) 117–123.
[26] C.-T. Leu, E. Luegmayr, L.P. Freedman, G.A. Rodan, A.A. Reszka, Bone 38 (2006) 628–636.
[27] Z.J. Henneman, G.H. Nancollas, F.H. Ebetino, R.G.G. Russell, R.J. Phipps, J. Biomed. Mater. Res. A 85A (2008) 993–1000.
[28] M.A. Lawson, Z. Xia, B.L. Barnett, J.T. Triffitt, R.J. Phipps, J.E. Dunford, R.M. Locklin, F.H. Ebetino, R.G.G. Russell, J Biomed Mater Res B Appl Biomater 92B (2009) 149–155.